PHILOSOPHICAL TRANSACTIONS A

royalsocietypublishing.org/journal/rsta

Opinion piece

Cite this article: Pritchard HD. 2026 How can we automate future gridded Antarctic ice-sheet and bed mapping? *Phil. Trans. R. Soc. A* **384**: 20250150.
https://doi.org/10.1098/rsta.2025.0150

Received: 9 July 2025
Accepted: 21 November 2025

One contribution of 16 to a Theo Murphy meeting issue 'Next generation ice-sheet bed measurements'.

Subject Areas:
glaciology, geophysics

Keywords:
ice sheet, ice shelf, Antarctic, Bedmap, sea level, survey

Author for correspondence:
Hamish D. Pritchard
e-mail: hprit@bas.ac.uk

How can we automate future gridded Antarctic ice-sheet and bed mapping?

Hamish D. Pritchard

British Antarctic Survey, Cambridge, UK

HDP, 0000-0003-2936-1734

As new airborne surveys of the Antarctic ice sheet are completed, the ever-enlarging survey dataset provides an opportunity for generating new 'Bedmaps' of ice thickness, surface and bed topography. These surveys are fundamental to improving our ability to predict the future of Antarctica, but other data-analysis challenges emerge because surveys often do not agree, large data gaps remain, the ice thickness changes or interpolation works well for one landscape but not another. Similar problems afflict other key Bedmap components: the coastline, the grounding line, rock outcrops, the ice shelves and the bathymetry. The process of merging the interpolated ice sheets and shelves and the grounded bed with the sea floor can also inject spurious cliffs and bumps in the grounding zone—exactly where ice-sheet models are most sensitive to flaws in their boundary conditions. In each case, unintended errors and artefacts that arise in the Bedmap grids require careful checking, correction and sometimes bespoke, local approaches to interpolation, slowing the process further. Here, I highlight the key challenges to overcome and address the question of how future Bedmaps can be automated to speed up the supply of new datasets demanded by the ice-sheet modelling community.

This article is part of the Theo Murphy meeting issue 'Next generation ice-sheet bed measurements'.

1. Introduction

Following the release of Bedmap3 [1], there remains an urgent need for compilations of the bed topography,

THE ROYAL SOCIETY PUBLISHING

surface topography and ice thickness of continental Antarctica and the surrounding Southern Ocean that take advantage of new surveys and the lengthening satellite record to increase the resolution, accuracy and timeliness of these datasets. Such products remain fundamental to the accuracy of projected sea-level rise, the effects of which threaten the lives and livelihoods of hundreds of millions of people living in, or dependent upon, the world's low-elevation coastal zones.

Until now, creating new versions of Bedmap has been relatively slow and labour-intensive, with products released only at decadal intervals (figure 1). To ensure ongoing and accelerated updates, a key question is: can future Bedmaps be automated? While desirable, the automation and frequent updating of Bedmap pose several challenges, both practical, in terms of data processing, and for the survey community, in terms of data sharing. Here, I discuss the challenges to overcome and possible solutions in automating, or at least accelerating, the 'bed-mapping' process.

2. Data sharing challenges

Since its inception, the Bedmap project has been reliant on the collection and contribution of new survey data at zero cost by a disparate community of researchers from multiple nations. This has been mutually beneficial to the surveyors, funders, Bedmap authors and users of its products by increasing the impact of the many separate regional and local survey activities that have fed into it and by providing compilations on a substantially larger scale than would otherwise be possible. This collaborative international framework therefore stands as a valuable Bedmap legacy and the foundation for future editions, but it also poses the challenge of how best to acknowledge and reward voluntary data contributions to the Bedmap data pool [2]. High-frequency updating of Bedmap products as new surveys are acquired is desirable for end users but would not favour the publication of associated 'benchmark' Bedmap papers whose high levels of interest and citation rates have so far incentivized co-authors to contribute data. At the time of writing, the Bedmap3 paper [1], for example, is in the 99th percentile of the 335 470 tracked articles of a similar age in all journals and the 99th percentile (ranked first) of the 261 tracked articles of a similar age in the journal *Scientific Data*. Similarly, the Bedmap2 paper [3] has been cited more than 2000 times, putting it in the top percentile of cited works in Earth science disciplines over the past decade. Because paper citations tend to be more valued than dataset downloads by science funders, this raises the risk that a smaller proportion of new datasets is freely and rapidly donated to the data pool. This risk is subject to the data sharing policies of the various funding bodies involved (for example, the Japan Science and Technology Agency, the US National Science Foundation, UK Research and Innovation, the European Commission and increasingly, the National Research Foundation of Korea, the National Natural Science Foundation of China and the Indian Department of Science and Technology require adherence to the findable, accessible, interoperable and reusable (FAIR) data sharing principles), and has yet to be tested, but for automated Bedmap, a new data agreement is required, and it is not obvious how to replace the existing incentive of citations in a model where new products are released frequently without an associated, high-impact paper.

3. Data analysis challenges

Conducting primary airborne, ground and ship surveys of the Antarctic bed remains the paramount challenge in Bedmapping, but compilation of the Bedmap suite of products also relies on multiple other, secondary datasets and data processing steps. Specifically, the Bedmap3 products define: the outer rock-and-ice coastline of Antarctica; the grounding line where ice goes afloat; areas of ice shelves that are transiently grounded; the extent and topography of rock outcrops; ice-sheet and ice-shelf thickness; ice and rock surface topography,

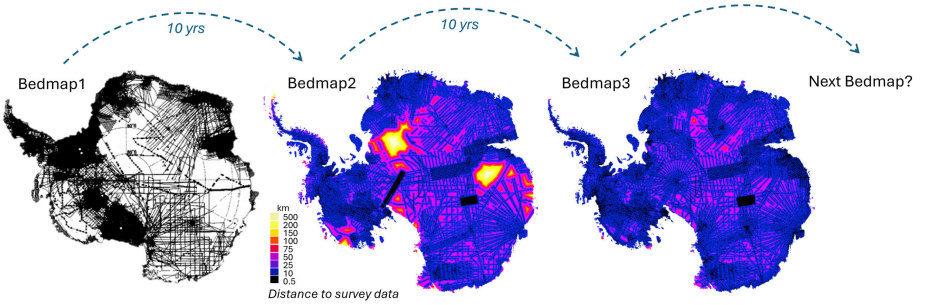

Figure 1. The production of previous Bedmaps has been driven by the progressive accumulation of survey data of ice-sheet thickness, with around a decade between recent iterations. Black points show data locations, the colour scale shows the improving distances to survey data from Bedmap2 to Bedmap3 as new missions were flown.

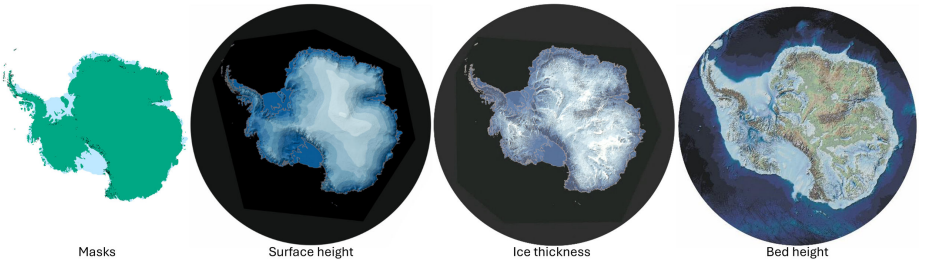

Figure 2. A Bedmap is not just an interpolated grid of ice thickness: it combines several mutually interdependent datasets.

the bed elevation of the grounded ice sheet, Lake Vostok, and the sea bed in sub-ice-shelf cavities, coastal seas and the open ocean (figure 2). Importantly, these factors *combined* are the key controls on ice flow that are fundamental to ice-sheet modelling, and therefore to predictions of future ice-sheet retreat or collapse and the resulting sea-level rise. Because they are physically interconnected, they co-vary: a change in the outer coastline owing to ice-shelf frontal retreat, for example, may lead to thinning and lowering of the ice shelf, the ungrounding of transient grounding zones, thinning and lowering of the grounded ice sheet and retreat of the grounding line, and it may imply local changes in the extent of exposed rock outcrops. Consequently, each new iteration of Bedmap needs to update, as much as possible, all these parameters simultaneously to a common era, so that the coastline, grounding line, etc., agree with the ice thickness distribution at that time. Furthermore, these definitions must comply with physical principles so that, for example, all cells classed as ice shelf have a surface height, thickness and sea-bed depth consistent with their being afloat, and all grounded ice cells at the coast have equivalent properties that conform with them not being afloat, and so on. Finally, when interpolating across grounding zones and adjusting cell values to pass these tests of physicality, the resulting distributions of surface height, thickness and bed height should vary smoothly (over scales of a few kilometres), avoiding abrupt, step-like artefacts between neighbouring cells over these important transitions in the gridded products (see also §3e). Failure to ensure that a new suite of Bedmap products is internally consistent in this way will lead to errors in the physical modelling of ice dynamics, and therefore errors in the projection of future ice-sheet change. These points apply regardless of the method used for interpolation of grounded ice thickness, whether through mass conservation (as in the related Bedmachine approach and products [4] or through spline fitting, as in Bedmap3).

As for the primary survey data, the supporting datasets needed to produce Bedmap grids are often limited in spatial or temporal extent and may be ambiguous, incomplete, outdated, inconsistent with other products or otherwise flawed. Previously, reconciling these imperfect datasets to create coherent and seamless Bedmap products has required numerous decisions to

be made and often manual editing to correct for their errors and deficiencies, which is a slow process. So, what are the key challenges in updating these various datasets, and can they be automated?

(a) Creating a new mask

The Bedmap mask grid (currently 54 million cells at 500 m spacing) depicts the extent of the features described above, which are key to defining the distribution of forces and drivers of change that affect ice dynamics and are important in determining how observational data are interpolated into the gridded products. The masks define, for example, the grounded areas of the ice sheet that experience basal drag versus ice-shelf areas that are free-floating and experience no drag, but are exposed to ocean-driven melting, and whose surface height (freeboard) can potentially be used to calculate ice-shelf thickness. As many of these features experience continuous change, the mask grid must be updated frequently.

(i) Updating the outer coastline mask

The Bedmap3 outer coastline is 61 000 km long, of which 24 000 km is made up of ice-shelf calving fronts, 22 000 km of grounded ice that meets the sea and 15 000 km of rock. This coastline was manually digitized from Landsat 8 images acquired during January–March 2022 [1], but because ice shelf and glacier fronts are in a continuous cycle of advance and calving and are prone to large and rapid changes in extent (figure 3), there is a strong case for automated coast mapping for future iterations.

To date, manual digitization (with optical or synthetic-aperture radar (SAR) satellite images) as used in Bedmap3 has been the main method for mapping ice fronts (85% of studies), but automated methods have been developed (7% of studies as of 2018) with notable advances through machine learning [6–8]. One largely automated 'elevation-edge' approach has successfully employed radar altimetry to detect and map the (tens of metres high) migrating front of the relatively thick Filchner–Ronne Ice Shelf [5]. In addition, a recently established operational service, IceLines, uses deep learning applied to SAR images to remap Antarctic ice shelves of at least 30 km width, plus six additional glacier fronts, on an ongoing monthly basis [9]. Challenges persist in distinguishing shelf ice from fast ice, mélange and icebergs, leading to mean positional errors of approximately 200–440 m depending on available images, and in some cases, automated front detection is at least temporarily unsuccessful, though aggregation of images over longer periods (e.g. 1 year) can provide near complete coverage of the targeted shelf fronts [9]. Covering 14 000 km of ice-shelf front, IceLines is, however, limited to only 30% of the outer coast of Antarctica made up of ice, and no approach has yet been applied to repeated automatic mapping of the remaining 32 000 km of coastline. Until recently, automatic mapping of the narrow, relatively steep, often ice-choked fronts of outlet glaciers that are common in, for example, the Antarctic Peninsula (e.g. figure 3*b*) has remained an intractable problem, but a deep learning approach has now been trialled successfully on 42 Antarctic Peninsula glacier fronts [8]. An obvious area for future development, therefore, lies in combining such deep learning approaches to cover the full extent of the glacierized Antarctic coast at approximately annual frequency.

(ii) Updating the grounding line mask

The Bedmap3 grounding line (between floating ice and grounded ice) is 54 000 km long and represents a manual reconciliation of the multiple, often incomplete, sometimes mutually incompatible grounding line mappings from various dates that were available at the time ([1]; figure 4). Disagreements may reflect different definitions of the grounding line (e.g. the inland limit of tidal flexure versus the most notable break in surface slope), or errors in the

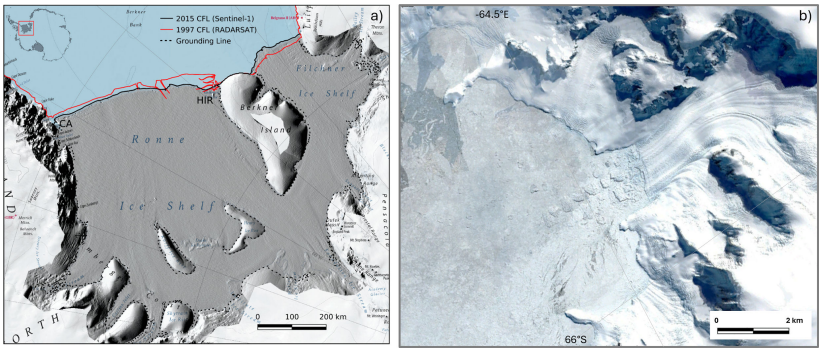

Figure 3. The outer calving front location (CFL) of (a) the changing Filchner Ronne Ice Shelf (from [5] (under licence CC BY)) and (b) a glacier on the Antarctic Peninsula with a complex, narrow calving front (from Google Earth).

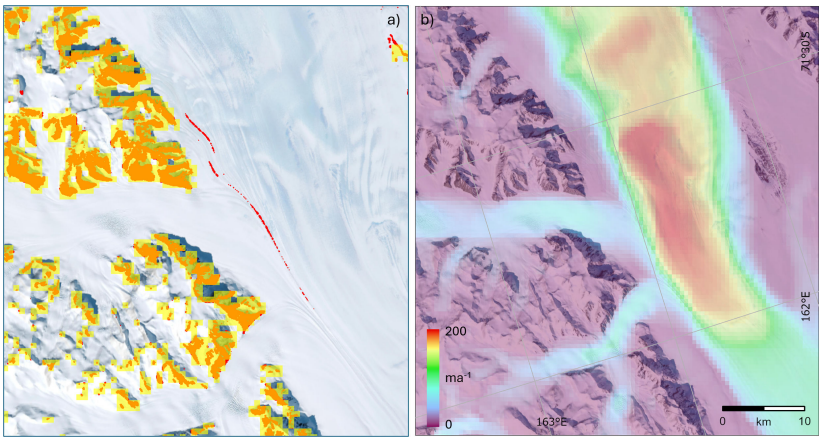

Figure 4. (a) Semi-transparent overlay of a sample of rock outcrops from the Bedmap3 gridded mask (yellow) overlain on ADD7.3 polygons (red) [10]. Orange shows where they coincide, red where ADD7.3 is more extensive, highlighting supraglacial moraine manually excluded in Bedmap3. (b) Ice flow rate for the area of Oates Land, East Antarctica, in (a) [11].

mappings, or sustained migration of the grounding line observed at different times, or tidal oscillation of the grounding line across the tidal grounding zone, sampled at different stages of the tide (e.g. [12]). Only one of the products available to Bedmap3 [13] reported grounding line positions that attempted to span the annual tidal range, but this record alone is not long enough to capture sustained migration and so represents a discrete snapshot of the grounding zone for the year 2018. Furthermore, gaps in grounding line products are common, largely resulting from a combination of limits to the orbital reach of the satellites used, limits to their spatial sampling (e.g. owing to wide track spacing) or poor signal-to-noise ratios, for example in detecting tide-induced flexure where tidal ranges are small and/or the surface changed rapidly owing to surface deformation or melt (e.g. figure 5).

Because the grounding line is known to be migrating at up to hundreds of metres per year in areas of ice loss ([18,19]; figure 5a), future Bedmap masks need to be updated frequently and preferably using a consistent definition, methods and temporal sampling around the continent. Furthermore, as grounding occurs across a zone up to 15 km wide defined by the tidal range, the local bed slope and the ice thickness gradient, rather than at a discrete line (e.g. [12]), it would be preferable to define this zone as a new class within future Bedmap mask grids (between, for example, the annual minimum and maximum tide, or one standard deviation from the mean tide or similar metric).

There are three remote sensing methods with the potential for automation and capable of large-scale, repeated grounding zone mapping: differential SAR interferometry (DInSAR),

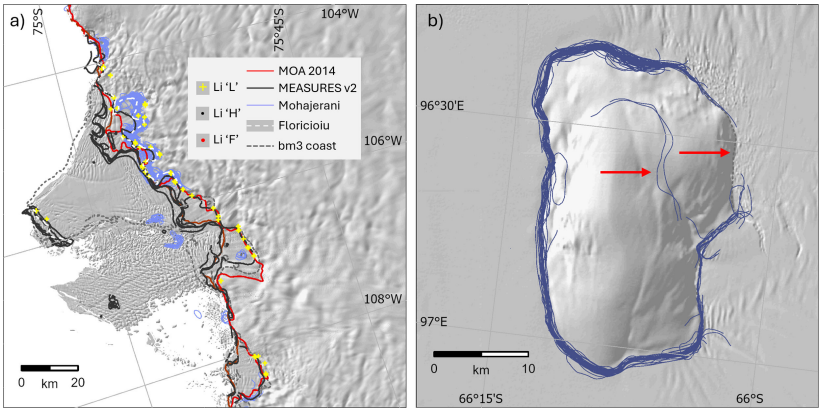

Figure 5. (a) Available grounding line mappings for Thwaites Glacier, West Antarctica, of varying date, location and extent showing evidence of both retreat (e.g. the MEASURES v. 2 lines are from 1992, 1994, 1996 and 2011 [14,15]) and tidal migration (partial coverage from 163 unique, automated 'Mohejerani' mappings spanning one year [13]). MOA 2014 refers to Haran *et al*. ([16]; updated 2019); Floricioiu refers to Floricioiu *et al*. [17]. (b) Automated 'Mohejerani' mapping of Masson Island (Shackleton Ice Shelf, western Mawson Sea) grounding lines (blue) showing gaps and errors (arrowed).

altimetry and feature tracking. DInSAR can provide spatially continuous and highly sensitive mapping of surface flexure and is the most accurate method for measuring the inland limit of grounding zone deformation. However, DInSAR satellites have had a limited orbital range of, for example, 77°S for Sentinel-1 that has excluded some grounding zones and, in many areas of rapid surface change, DInSAR suffers from coherence loss that has further prevented grounding zone mapping (e.g. [19]; explaining the limited extent of the Sentinel-1 derived 'Moherjerani' lines in figure 5a).

The COSMO-SkyMed constellation now extends the orbital limit to approximately 80°S, and recent advances in automated processing of wrapped DInSAR interferograms through both physical modelling of tidal flexure (the 'phase gradient' method) and deep learning can improve both the accuracy of grounding zone mapping and its robustness to noise [13,18,20]. Using COSMO-SkyMed data over five large Antarctic outlet glaciers, Ross *et al*. [18] found the automated phase gradient approach to be suited to approximating the grounding line location, while the neural network approach achieved higher precision but remains poorly suited to high-priority but 'low-coherence, high-complexity areas like those found in the glaciers at the Amundsen Sea Embayment' of West Antarctica. Automated DInSAR, therefore, offers only a partial solution to future grounding zone mapping.

Alternatively, repeat-track ICESat-2 altimetry can be used to detect the transition from tidal to grounded ice and has a high orbital limit of 88°S, but observes a sample of points along tracks that can be separated by hundreds of metres rather than providing spatially continuous mapping (like DInSAR), has a repeat period of 91 days, limiting its temporal sampling of the tidal cycle and has not yet been automated for widespread use [12]. It has been found to perform well along the Siple Coast, where sampling is dense, but less well in areas with frequent cloud cover, heavy crevassing, melt ponds and sparser track spacing, characteristic of the Antarctic Peninsula and Amundsen Sea Embayment, and where orbital tracks are not perpendicular to the grounding zone (e.g. [21,22]). This implies that altimetry can similarly offer only a partial solution to grounding zone mapping but may complement the coverage of DInSAR.

The feature tracking approach was specifically developed for use where DInSAR coherence is low; it can operate independently of cloud cover and can produce locally continuous grounding zone maps [19]. It detects tide-induced anomalies in tracked surface flow rate (supported by a tide model of expected flexure) and has been demonstrated to work well using Sentinel-1 SAR images on Antarctic Peninsula ice shelves, including Flask and Leppard glaciers,

the SCAR Inlet and even around the George VI Ice Shelf where the tidal range is relatively small, suggesting that it could be applied across most of coastal Antarctica [19]. However, it works less reliably where the ice shelf is not free-floating and so shelf flexure does not conform well to available tide models (e.g. close to the grounding zone of thick ice shelves and ice streams), and with its relatively poor signal-to-noise ratio, is less precise and less accurate than DInSAR, displaying a systematic seaward bias of typically up to a few hundred metres, and a quoted accuracy of ±490 m [19]. However, the use of an elastic or visco-elastic beam model to improve estimates of ice-shelf tidal flexure could, in future, improve the accuracy of this approach [19], and if implemented in parallel, this tracking method could fill many of the gaps left by DInSAR and altimetry for automated and frequent mapping of the Antarctic grounding zone.

(iii) Updating the rock outcrop mask

The Bedmap3 mask includes around 26 000 discrete rock outcrops occupying approximately 300 000 cells that originated from the Antarctic Digital Database 7.3 (ADD7.3), and in most areas were mapped automatically from optical satellite images [10]. Outcrops provide valuable constraints for ice thickness or bed interpolation, particularly where survey data are lacking, and while most change little through time, their extent is prone to change where ice is retreating, prompting a need for periodic remapping. Automated classification of rock in satellite images is well established, but can fail to distinguish between bedrock outcrops and supraglacial moraine that can overlie ice of considerable thickness (e.g. figure 4). Misinterpretation of moraine as bedrock can therefore severely bias interpolation of ice thickness and bed topography.

For Bedmap3, we manually checked the ADD7.3 outcrops against satellite images to identify and remove supraglacial moraine from the rock mask, but the challenge for future iterations is to automate this step. Automated detection of supraglacial moraine could employ testing for: non-zero surface flow rate or highly elongated, linear features (e.g. figure 4); lower interferometric coherence than bedrock owing to the greater mobility of moraine; a greater thermal lag of moraine overlying ice (e.g. [23]) or contrasts with bedrock in near- and short-wave infrared spectral signatures in response to contrasts in their moisture content (e.g. [24]). Automated supraglacial debris mapping using multiple sources of remote sensing, topographic data and deep learning has been demonstrated for the Himalayas and Karakoram [25], and optical and infrared remote sensing has been applied for most areas globally; hence, there is potential for automation, but this has not yet been applied to the Greenland and Antarctic ice sheets [26].

(b) Quality controlling ice thickness data

The masks of floating and grounded ice determine the extent to which survey data (for grounded ice thickness) and altimetry-derived datasets (for ice-shelf thickness) can be employed for thickness interpolation, and these distinct data sources have differing requirements for quality control before they can be interpolated and merged into a continuous grid of ice thickness.

(i) Grounded ice survey data

Where survey lines cross, disagreements in ice thickness between surveys are common and can reach hundreds of metres [1]. This becomes particularly apparent after interpolation, as anomalous points or tracks introduce steps, spikes or pits into the interpolated thickness grid (and subsequently the bed topography grid; figure 6a). Potential causes include positional errors in older surveys, mis-picked bed horizons in radargrams, differing radar velocities used

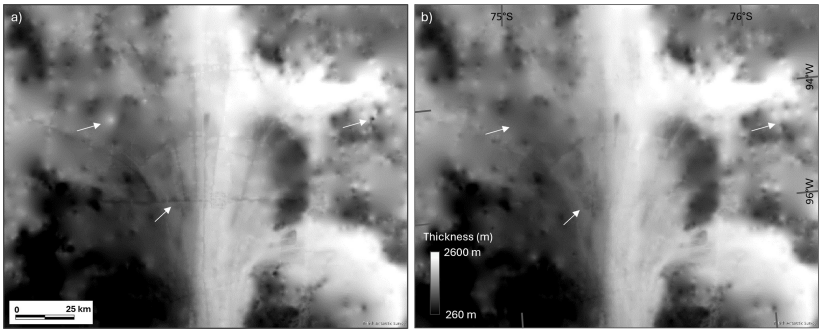

Figure 6. (a) Preliminary ice thickness interpolation of unedited Bedmap3 survey data over the main trunk of Pine Island Glacier, West Antarctica. (b) Final Bedmap3 ice thickness grid after manual, localized cross-calibration and cleaning of survey data over the areas shown in (a). Arrows highlight the location of notable artefacts in (a).

to convert from signal travel time to depth, changes in the column-averaged density of the ice sheet and actual changes in ice thickness between visits.

Bedmap3 employed 1.9 million line-kilometres of survey data converted into 3.64 million 'summarized points'. After several iterations of preliminary thickness interpolation, we culled 8% of these points and, for areas with well-known thickness change over time, we calibrated older, biased tracks to agree with more recent surveyed thicknesses at crossovers [1]. This quality control process removed prominent anomalies in gridded thickness (e.g. figure 6b), but in the absence of objective information on survey data accuracy, this remains a subjective and laborious process.

To automate the data culling step described above, locally adaptive filters could be designed to remove outlier data points or lines, a process that could be iterated to achieve a subjectively better final product. However, this would still require judgement by the user; its effectiveness would vary with the density of survey data within a given neighbourhood, and ambiguity is likely to persist between surveys of similar extent and density whose measurements disagree. This implies that automation could be relatively simply achieved, but with the risk of excluding valid data or failing to exclude all invalid data; hence, manual intervention may still be required in the quality control step.

To overcome the calibration problem of ice thickness changes between surveys, interpolation over the grounded ice sheet could in future be done not with the thickness values (as in previous Bedmaps) but with absolute bed elevation, because these should remain largely unchanged over the relevant time scales. It would yield a consistent map of bed topography regardless of survey date, which, appealingly, could be subtracted from a surface digital elevation model (DEM) of a chosen date to yield a grounded ice thickness grid representing that chosen date. This would, however, require an accurate absolute surface elevation for each point in addition to the measured thickness value, either from the original survey or a contemporaneous surface DEM. An accurate elevation is likely to be available for surveys within approximately the last 30 years (with differential GPS and continent-wide, high-resolution satellite altimetry) and for all future survey data, though the quality of surface elevations in existing surveys has not been assessed by the Bedmap project, and this approach would exclude surveys older than approximately 30 years, including much of the data contributed to Bedmap1 (figure 1a). If surface elevations prove adequate, this change could avoid the need to automate inter-survey thickness calibration.

(ii) Ice-shelf freeboard data

Around 300 ice shelves fringe the Antarctic coast, many with no thickness survey measurements and some experiencing rapid thickness change. For consistency in date, method and coverage, Bedmap3 employed a satellite-altimetry derived thickness dataset covering 92% of the

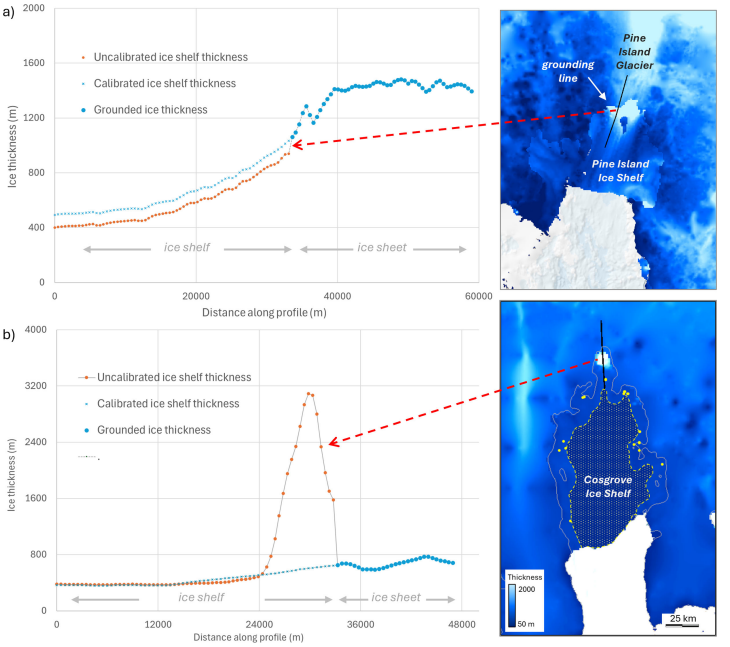

Figure 7. (a) Example of ice-shelf thickness calibration (from the orange to blue points), leading to the removal of a step artefact in ice thickness at the Pine Island Glacier grounding line. (b) A 2500 m ice bulge artefact in shelf thickness owing to failure of the hydrostatic-equilibrium assumption (graph, orange points and map, white patch). Yellow dots on the map show independent mapping of the 'hydrostatic limit' [28]. The yellow dashed line and hatched area show the manually edited area of valid altimetry-derived shelf thicknesses. The blue points in the graph show the interpolated thickness after exclusion of the bulge.

ice-shelf area that estimated thickness from freeboard based on an estimated column-averaged density and an assumption that the mapped areas are in hydrostatic equilibrium [27]. Testing against approximately 400 000 summarized survey points revealed spatially coherent bias in freeboard-derived thickness of up to approximately 150 m related to errors in assumed density, which we corrected for where possible ([1]; e.g. figure 7a). In some areas incorrectly assumed to be in hydrostatic equilibrium, we also identified large and variable positive thickness biases of tens to thousands of metres (e.g. figure 7b) by comparison with survey data on the shelves and from marked contrasts in thickness relative to the adjacent grounded ice sheet. We cropped these out manually, guided where possible by the hydrostatic limit identified elsewhere [28], and then interpolated across these extended gaps to ensure a smooth thickness transition between shelf and grounded ice (figure 7b).

An ongoing supply of altimetry data (including ICESat-2, CryoSat-2, Sentinel-3A and 3B and upcoming missions CRISTAL and Sentinel-6B) and firn density modelling (e.g. RACMO2.3 [29]) supports the automation of future altimetry-based ice-shelf thickness mapping, and an automated calibration step using contemporaneous surveys of shelf thickness, where available, could reasonably be built into this processing chain. In addition, non-hydrostatic shelf areas could be excluded automatically provided that the hydrostatic limit (based on tidal flexure observations) is mapped comprehensively around the Antarctic grounding zone and updated to capture migration owing to shelf thickness changes. However, while a snapshot of flexure limits is currently available in some areas, comprehensive and updated hydrostatic mapping is not. Automation of this process, therefore, depends upon progress in grounding zone mapping (§3a(ii)).

(c) Synthesizing additional ice thickness data

(i) Streamlines

Unless specifically designed to follow known subglacial troughs, Antarctic survey patterns tend to capture poorly the longitudinal form of troughs eroded into the subglacial landscape by ice flow (figure 8a). With spline-based interpolation [1], troughs can appear 'beaded' rather than the smoothly continuous features familiar from deglaciated landscapes (e.g. figure 8d). Interpolation by mass conservation techniques can effectively interpolate a realistic trough shape between surveyed flux gates, provided that there is detectable surface flow along the trough [4], but not in slow-flowing areas common in the ice-sheet interior (e.g. figure 8b). Instead, patterns in the survey data themselves (supported by, for example, patterns in visible surface texture) can be used to guide the interpolation. For Bedmap3, we visually identified patterns of maxima in ice thickness that aligned across multiple adjacent survey lines to indicate the course of a subglacial trough, and we manually digitized around 5000 'streamlines' linking these points. These digitized streamlines are analogous to the river linking the topographic minima of the cross profiles in figure 8a, and we used these to enforce linear thickness interpolation along the trough floor between adjacent surveyed values, to produce smooth, continuous, subjectively more realistic glacial trough features (figure 8e versus 8*d*).

As more surveys are conducted, there will be further opportunities to modify and add to this collection of streamlines, and this could potentially be automated by an algorithm that searches and links sequences of thickness maxima/topographic minima, perhaps similar to automated radargram layer picking (e.g. [30,31]), and potentially supported by pattern detection in surface texture and flow (e.g. [32]).

(ii) Creep flow around rock outcrops

Rock outcrops provide useful constraints for thickness interpolation (§3a(iii)), but areas of typically thin, slow-flowing ice around outcrops are often poorly surveyed for thickness. Among mountain ranges in particular, numerous rock outcrops exist that are known to be separated by slow-flowing ice but with no thickness measurements between them. Interpolation in such settings tends, therefore, to populate these gaps with thicknesses biased towards zero.

To overcome this thin bias, in Bedmap3, we estimated the thickness of slow-flowing, relatively steep ice around outcrops using Glen's flow law for non-sliding creep flow (e.g. fig. 5 in [1]), which provided physically based thickness estimates for approximately 750 000 cells. These spatially distributed calculations required high-resolution maps of surface flow speed [14] and slope (after [33]), plus an Antarctic-wide map of mean annual temperature (after [34]) and firn-air-content [4]. As improved maps of these parameters become available or mapping at a higher resolution is required, these thin-ice estimates would be relatively straightforward to automate. Frequent updating is unlikely to be necessary given that the slow-flowing ice around such outcrops is unlikely to experience rapid change.

(d) Updating circum-Antarctic bathymetry

The bathymetry of Antarctica's continental shelf acts as a key control on ice–ocean interactions and ocean forcing of ice-sheet retreat, but large areas, particularly in the marine cavities below the ice shelves, remain among the least well surveyed areas on Earth [35]. For Bedmap3 bathymetry, we relied primarily on the IBCSOv2 compilation [36], updated with more recently released, local compilations in two areas of the continental shelf near the Nivl and Totten ice shelves of East Antarctica (around 10°E and 116°E, respectively). Since then, a major new compilation based on inversion of gravity data has been released that substantially updates

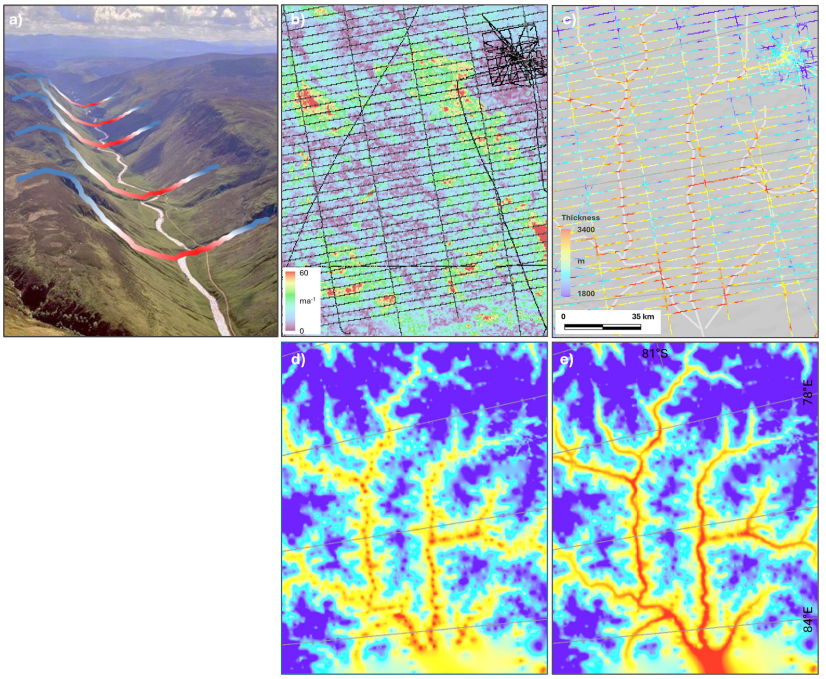

Figure 8. (a) Illustrative survey line cross profiles over a deglaciated trough, with blue to red indicating relative topography (or thickness of an overlying ice sheet). The trough floor has a smoothly continuous long profile which the river flows down; (b) survey flightlines and surface flow rate [14] over the Gamburtsev Subglacial Highlands, East Antarctica; (c) survey thicknesses (colour scale) and manually digitized 'streamlines' (white) linking adjacent survey-line points of maximum thickness; (d) spline-interpolated thickness (colour scale in (c)) without streamlines; (e) Bedmap3 interpolated thickness with streamlines. Panels (b–e) all show the same extent.

Antarctic-wide sub-ice-shelf bathymetry and identifies numerous, previously unmapped troughs [37], an advance that will improve future Bedmappings. However, the accuracy of such inversions remains critically dependent on the availability of high-quality and extensive gravity surveys (typically from aircraft) and, to constrain the inversion, direct bathymetry measurements from ice shelves, which remain scarce [38]—there is therefore considerable scope to improve the accuracy, resolution and uncertainty quantification of mapping in these areas through new surveys [37,38]. As such, an automated processing chain to rerun a gravity inversion algorithm as new measurements become available could make a particularly valuable contribution to automated Bedmapping.

(e) Merging thickness and bed grids

After separately gridding the ice sheet and shelf thickness and the grounded and sea-bed topography, two steps follow that are key to the success of the new Bedmap products as boundary conditions for ice-sheet models: the smooth (near-seamless) merging of the ice sheet with the ice shelves and of the grounded bed with the sea bed, over length scales of a few kilometres seaward of the grounding line. Because of their different origins (and notably the failure of freeboard-based thickness estimates and the paucity of bathymetry observations in this zone), crude mosaicking of these grids is prone to introducing abrupt step artefacts in thickness and bed between adjacent cells either side of the grounding line (e.g. fig. 10 in [1]), which should be avoided. If sufficient ice thickness survey data spanning the grounding zone are available for a suitable common epoch (uncontaminated by real changes in thickness through time), then these could allow the ice thickness transition to be mapped explicitly, but this is rarely the case.

The adaptive spline-fitting interpolation algorithm used in Bedmap3 is well suited to achieving smooth transitions between grids if a gap is left between them sufficiently large to allow the splines to conform smoothly to the offset and local curvature of the two grids on either side. We imposed a default 3 km gap in thickness grids and 10 km gap in bed grids seaward of the grounding line but extended these case-by-case where visual inspection showed that these were insufficient to achieve a smooth transition [1]. In the absence of suitable sub-ice-shelf observations, the detailed bathymetry of, for example, a grounding zone wedge, is not explicitly depicted in this approach, but the smoothly dipping, kilometres-scale long profiles of such features are relatively spline-like (e.g. [39]) and hence can at least be approximated in this way.

This labour-intensive visual inspection and refinement of the merge process could potentially be automated by an algorithm that searches for deviations in the ice thickness gradient or the bed slope offshore of the grounding line that persist after interpolation across the 3 or 10 km gap, respectively, and that locally increases this gap and re-interpolates iteratively until the transition is acceptably smooth. This algorithm is yet to be developed, however, and the definition of an 'acceptably smooth' transition is subjective and very likely to differ across the range of landscapes between, for example, the narrow and steep-sided fjords and gently sloping coastal plains of the 54 000 km grounding line. Consequently, automation of this merge process is unlikely to be trivial.

Finally, the test for 'physicality' of the combined surface height, merged ice thickness, merged bed height, water column thickness and mask status as floating or grounded must be applied (all cells classed as ice shelf have a surface height, thickness and sea-bed depth consistent with their being afloat, all grounded ice cells at the coast have equivalent properties that conform with them not being afloat, all sea bed cells lie below sea level, etc.; [1]). In itself, this test of physical rules could readily be automated, but the (automated) adjustment of non-physical cells to meet these rules can then introduce new step-like artefacts in the transition zones described above, prompting further iterations to the 'transition-smoothing' and 'physicality-testing' processes. This adds somewhat to the challenge of automatic merging of the thickness and bed grids.

4. Conclusions

Automation of future Bedmaps is desirable, but this is not trivial because the Bedmap grids are co-dependent and should be updated together in a way that obeys physical rules. In addition to new ice thickness survey data, each Bedmap grid relies upon multiple supporting datasets that have their own limitations in coverage, accuracy and timeliness. Hence, while it is relatively easy to produce a new Bedmap that is superficially more complete than the last as new surveys are conducted, it is more complex to ensure that each new suite of products meet the needs of ice-sheet models. There is, however, considerable scope for accelerating the Bedmap process through automation of key steps, notably in the remapping of the outer coastline, grounding zone and ice-shelf thickness and in automating the quality control process for the resulting grids. A promising theme in progress towards automation is the increasing use of machine learning, including deep learning and neural networks, to replace labour-intensive manual mapping.

Data accessibility. The Bedmap3 datasets are available in [40]. The Bedmachine datasets are available at: https://nsidc.org/data/nsidc-0756. Ice-flow datasets are available at: https://nsidc.org/data/nsidc-0484/versions/2. Ice-shelf cavity bathymetry data are available in [41].

Declaration of AI use. I have not used AI-assisted technologies in creating this article.

Authors' contributions. H.P.: conceptualization, data curation, investigation, methodology, validation, visualization, writing—original draft.

Conflict of interest declaration. I declare I have no competing interests.
Funding. No funding has been received for this article.
Acknowledgements. H.D.P. was employed by the UK Natural Environment Research Council while conducting this work.

References

1. Pritchard HD *et al*. 2025 Bedmap3 updated ice bed, surface and thickness gridded datasets for Antarctica. *Sci. Data* **12**, 414. (doi:10.1038/s41597-025-04672-y)
2. Frémand AC *et al*. 2023 Antarctic bedmap data: findable, accessible, interoperable, and reusable (FAIR) sharing of 60 years of ice bed, surface, and thickness data. *Earth Syst. Sci. Data* **15**, 2695–2710. (doi:10.5194/essd-15-2695-2023)
3. Fretwell P *et al*. 2013 Bedmap2: improved ice bed, surface and thickness datasets for Antarctica. *Cryosphere* **7**, 375–393. (doi:10.5194/tc-7-375-2013)
4. Morlighem M *et al*. 2020 Deep glacial troughs and stabilizing ridges unveiled beneath the margins of the Antarctic ice sheet. *Nat. Geosci.* **13**, 132–137. (doi:10.1038/s41561-019-0510-8)
5. Wuite J, Nagler T, Gourmelen N, Escorihuela MJ, Hogg AE, Drinkwater MR. 2019 Sub-annual calving front migration, area change and calving rates from swath mode cryosat-2 altimetry, on filchner-ronne ice shelf, Antarctica. *Remote Sens.* **11**, 2761. (doi:10.3390/rs11232761)
6. Baumhoer CA, Dietz AJ, Dech S, Kuenzer C. 2018 Remote sensing of Antarctic glacier and ice-shelf front dynamics—a review. *Remote Sens.* **10**, 1445. (doi:10.3390/rs10091445)
7. Heidler K, Mou L, Loebel E, Scheinert M, Lefèvre S, Zhu XX. 2023 A deep active contour model for delineating glacier calving fronts. *IEEE Trans. Geosci. Remote Sens.* **61**, 1–12. (doi:10.1109/tgrs.2023.3296539)
8. Loebel E, Baumhoer CA, Dietz A, Scheinert M, Horwath M. 2025 Calving front positions for 42 key glaciers of the Antarctic Peninsula ice sheet: a sub-seasonal record from 2013 to 2023 based on deep-learning application to Landsat multi-spectral imagery. *Earth Syst. Sci. Data* **17**, 65–78. (doi:10.5194/essd-17-65-2025)
9. Baumhoer CA, Dietz AJ, Heidler K, Kuenzer C. 2023 IceLines - a new data set of Antarctic ice shelf front positions. *Sci. Data* **10**, 138. (doi:10.1038/s41597-023-02045-x)
10. Gerrish L. 2020 Automatically extracted rock outcrop dataset for Antarctica (7.3). [Data set]. UK Polar Data Centre, Natural Environment Research Council, UK Research and Innovation. ()
11. Gardner A, Fahnestock M, Scambos T. 2022 MEaSUREs ITS_LIVE Regional Glacier and Ice Sheet Surface Velocities. (NSIDC-0776, Version 1). [Data Set]. Boulder, Colorado USA. NASA National Snow and Ice Data Center Distributed Active Archive Center. doi.org/10.5067/6II6VW8LLWJ7.
12. Freer BID, Marsh OJ, Hogg AE, Fricker HA, Padman L. 2023 Modes of Antarctic tidal grounding line migration revealed by Ice, Cloud, and land Elevation Satellite-2 (ICESat-2) laser altimetry. *Cryosphere* **17**, 4079–4101. (doi:10.5194/tc-17-4079-2023)
13. Mohajerani Y, Jeong S, Scheuchl B, Velicogna I, Rignot E, Milillo P. 2021 Automatic delineation of glacier grounding lines in differential interferometric synthetic-aperture radar data using deep learning. *Sci. Rep.* **11**, 4992. (doi:10.1038/s41598-021-84309-3)
14. Mouginot J, Scheuchl B, Rignot E. 2017 MEaSUREs Annual Antarctic Ice Velocity Maps. (NSIDC-0720, Version 1). [Data Set]. Boulder, Colorado USA. NASA National Snow and Ice Data Center Distributed Active Archive Center. ()
15. Rignot E, Mouginot J, Scheuchl B. 2022 MEaSUREs Grounding Zone of the Antarctic Ice Sheet. (NSIDC-0778, Version 1). [Data Set]. Boulder, Colorado USA. NASA National Snow and Ice Data Center Distributed Active Archive Center. ()
16. Haran T, Bohlander J, Scambos T, Painter T, Fahnestock M. 2014 MODIS Mosaic of Antarctica 2008-2009 (MOA2009) Image Map. (NSIDC-0593, Version 2). [Data Set]. Boulder, Colorado USA. NASA National Snow and Ice Data Center Distributed Active Archive Center. ()

17. Floricioiu D, Krieger L, Chowdhury TA, Bässler M. 2021 ESA Antarctic ice sheet climate change initiative (Antarctic_ice_sheet_cci): grounding line location for key glaciers, Antarctica, 1994-2020, v2.0, NERC EDS centre for environmental data analysis. See https://catalogue.ceda.ac.uk/uuid/7b3bddd5af4945c2ac508a6d25537f0a.
18. Ross N, Milillo P, Dini L. 2024 Automated grounding line delineation using deep learning and phase gradient-based approaches on COSMO-SkyMed DInSAR data. *Remote Sens. Environ.* **315**, 114429. (doi:10.1016/j.rse.2024.114429)
19. Wallis BJ, Hogg AE, Zhu Y, Hooper A. 2024 Change in grounding line location on the Antarctic Peninsula measured using a tidal motion offset correlation method. *Cryosphere* **18**, 4723–4742. (doi:10.5194/egusphere-2023-2874)
20. Parizzi A. 2020 Potential of an automatic grounding zone characterization using wrapped InSAR Phase. In *IGARSS 2020 - 2020 IEEE Int. Geoscience and Remote Sensing Symposium*. (doi:10.1109/igarss39084.2020.9323199)
21. Li T, Dawson GJ, Chuter SJ, Bamber JL. 2023 Grounding line retreat and tide-modulated ocean channels at Moscow University and totten glacier ice shelves, East Antarctica. *Cryosphere* **17**, 1003–1022. (doi:10.5194/tc-17-1003-2023)
22. Freer BID, Marsh OJ, Fricker HA, Hogg AE, Siegfried MR, Floricioiu D, Sauthoff W, Rigby R, Wilson SF. 2024 Coincident lake drainage and grounding line retreat at engelhardt Subglacial Lake, West Antarctica. *J. Geophys. Res.* **129**, e2024JF007724. (doi:10.1029/2024jf007724)
23. Mihalcea C, Brock BW, Diolaiuti G, D'Agata C, Citterio M, Kirkbride MP, Cutler MEJ, Smiraglia C. 2008 Using ASTER satellite and ground-based surface temperature measurements to derive supraglacial debris cover and thickness patterns on Miage Glacier (Mont Blanc Massif, Italy). *Cold Reg. Sci. Technol.* **52**, 341–354. (doi:10.1016/j.coldregions.2007.03.004)
24. Singh DK, Thakur PK, Naithani BP, Kaushik S. 2021 Quantifying the sensitivity of band ratio methods for clean glacier ice mapping. *Spat. Inf. Res.* **29**, 281–295. (doi:10.1007/s41324-020-00352-8)
25. Kaushik S, Singh T, Bhardwaj A, Joshi PK, Dietz AJ. 2022 Automated delineation of supraglacial debris cover using deep learning and multisource remote sensing data. *Remote Sens.* **14**, 1352. (doi:10.3390/rs14061352)
26. Scherler D, Wulf H, Gorelick N. 2018 Global assessment of supraglacial debris - cover extents. *Geophys. Res. Lett.* **45**, 798–711. (doi:10.1029/2018gl080158)
27. Dawson GJ, Bamber JL. 2017 Antarctic grounding line mapping from CryoSat - 2 radar altimetry. *Geophys. Res. Lett.* **44**, 886–811. (doi:10.1002/2017GL075589)
28. Li T, Dawson GJ, Chuter SJ, Bamber JL. 2022 A high-resolution Antarctic grounding zone product from ICESat-2 laser altimetry. *Earth Syst. Sci. Data* **14**, 535–557. (doi:10.5194/essd-14-535-2022)
29. van Wessem JM, Reijmer CH, Lenaerts JTM, van de Berg WJ, van den Broeke MR, van Meijgaard E. 2014 Updated cloud physics in a regional atmospheric climate model improves the modelled surface energy balance of Antarctica. *Cryosphere* **8**, 125–135. (doi:10.5194/tc-8-125-2014)
30. Sime LC, Karlsson NB, Paden JD, Prasad Gogineni S. 2014 Isochronous information in a greenland ice sheet radio echo sounding data set. *Geophys. Res. Lett.* **41**, 1593–1599. (doi:10.1002/2013gl057928)
31. Moqadam H, Steinhage D, Wilhelm A, Eisen O. 2025 Going deeper with deep learning: automatically tracing internal reflection horizons in ice sheets—methodology and benchmark data Set. *J. Geophys. Res.* **2**, e2024JH000493. (doi:10.1029/2024JH000493)
32. Ockenden H, Bingham R, Goldberg D, Curtis A. 2024 Antarctic subglacial topography mapped from space reveals complex mesoscale landscape dynamics. *PREPRINT (Version 1) available at Research Square*. (doi:10.21203/rs.3.rs-4355387/v1)
33. Dong Y, Zhao J, Li C, Liao M. 2022 Gapless-REMA100: a gapless 100-m reference elevation model of Antarctica with voids filled by multi-source DEMs. *ISPRS J. Photogramm. Remote Sens.* **186**, 70–82. (doi:10.1016/j.isprsjprs.2022.01.024)
34. Copernicus Climate Change Service. 2023 ERA5 monthly averaged data on single levels from 1940 to present. Copernicus Climate Change Service (C3S) Climate Data Store (CDS). (doi:10.24381/cds.f17050d7)

35. Pritchard HD. 2014 Bedgap: where next for Antarctic subglacial mapping? *Antarct. Sci.* **26**, 742–757. (doi:10.1017/s095410201400025x)
36. Dorschel B *et al*. 2022 The international bathymetric chart of the Southern Ocean version 2 (IBCSO v2), PANGAEA.
37. Charrassin R, Millan R, Rignot E, Scheinert M. 2025 Bathymetry of the Antarctic continental shelf and ice shelf cavities from circumpolar gravity anomalies and other data. *Sci. Rep.* **15**, 1214. (doi:10.1038/s41598-024-81599-1)
38. Tankersley MD, Horgan H, Caratori-Tontini F, Tinto K. 2025 Gravity Inversion for sub-ice shelf bathymetry: strengths, limitations, and insights from synthetic modeling. *EGUsphere* **2025**, 1–53. (doi:10.5194/egusphere-2025-2380)
39. Batchelor CL, Dowdeswell JA. 2015 Ice-sheet grounding-zone wedges (GZWs) on high-latitude continental margins. *Mar. Geol.* **363**, 65–92. (doi:10.1016/j.margeo.2015.02.001)
40. Pritchard H *et al*. 2024 BEDMAP3 - Ice thickness, bed and surface elevation for Antarctica - gridding products (Version 1.0) [Data set]. NERC EDS UK Polar Data Centre. (doi:10.5285/2d0e4791-8e20-46a3-80e4-f5f6716025d2)
41. Rignot E, Millan R, Charrassin R, Scheinert M. 2024 Bathymetry of the Antarctic continental shelf and ice shelf cavities from a 3D inversion of circumpolar gravity anomalies constrained by other data. Dryad Digital Repository. (doi:10.5061/dryad.rbnzs7hkc)